Inactivation of FGF8 in early mesoderm reveals an essential role in kidney development

Alan O. Perantoni[1], Olga Timofeeva[1,*], Florence Naillat[3,*], Charmaine Richman[2], Sangeeta Pajni-Underwood[2], Catherine Wilson[2], Seppo Vainio[3], Lee F. Dove[1] and Mark Lewandoski[2,†]

[1]Laboratory of Comparative Carcinogenesis, National Cancer Institute, NCI-Frederick, Frederick, MD 21702, USA
[2]Cancer and Developmental Biology Laboratory, National Cancer Institute, NCI-Frederick, Frederick, MD 21702, USA
[3]Biocenter Oulu and Department of Medical Biochemistry and Molecular Biology, University of Oulu, PO Box 5000, FIN-90014 Oulu, Finland

*These authors contributed equally to this work
†Author for correspondence (e-mail: mlewandoski@mail.ncifcrf.gov)

Accepted 17 June 2005

Development 132, 3859-3871
Published by The Company of Biologists 2005
doi:10.1242/dev.01945

Summary

To bypass the essential gastrulation function of *Fgf8* and study its role in lineages of the primitive streak, we have used a new mouse line, T-Cre, to generate mouse embryos with pan-mesodermal loss of *Fgf8* expression. Surprisingly, despite previous models in which *Fgf8* has been assigned a pivotal role in segmentation/somite differentiation, *Fgf8* is not required for these processes. However, mutant neonates display severe renal hypoplasia with deficient nephron formation. In mutant kidneys, aberrant cell death occurs within the metanephric mesenchyme (MM), particularly in the cortical nephrogenic zone, which provides the progenitors for recurring rounds of nephron formation. Prior to mutant morphological changes, *Wnt4* and *Lim1* expression, which is essential for nephrogenesis, is absent in MM. Furthermore, comparative analysis of *Wnt4*-null homozygotes reveals concomitant downregulation of *Lim1* and diminished tubule formation. Our data support a model whereby FGF8 and WNT4 function in concert to induce the expression of *Lim1* for MM survival and tubulogenesis.

Key words: Cre recombinase, *Fgf8*, Kidney, *Lim1*, Nephron, Somitogenesis, T-Cre, *Wnt4*, Mouse

Introduction

Fibroblast growth factors (FGFs) play a role in numerous key developmental events, such as gastrulation and organogenesis including somite, brain and limb development. Efforts to delineate the tissue-specific roles of individual FGF genes are sometimes complicated by the fact that different members of this 22 gene family play partially redundant roles in the same tissue (Boulet et al., 2004; Sun et al., 2002; Xu et al., 2000) and that specific FGF genes are required in different embryonic tissues at various stages of development (Meyers et al., 1998; Ornitz and Itoh, 2001). *Fgf8* falls into both of these categories.

Fgf8 is first expressed in the pre-gastrulation epiblast and then in the primitive streak (Crossley and Martin, 1995). Gastrulation fails in $Fgf8^{-/-}$ embryos (Sun et al., 1999). To bypass this gastrulation requirement, mice carrying *Fgf8* hypomorphic alleles or tissue-specific gene inactivations have been studied. In the midbrain-hindbrain boundary, *Fgf8* inactivation results in aberrant cell death of the prospective midbrain and cerebellum (Chi et al., 2003; Meyers et al., 1998), whereas later cerebellar development requires both FGF8 and FGF17 (Xu et al., 2000). In the first branchial arch, *Fgf8* inactivation causes abnormalities in cardiovascular and smooth muscle development, mandibles, the submandibular salivary gland and teeth (Abu-Issa et al., 2002; Macatee et al., 2003; Trumpp et al., 1999). In the limb bud, apical ectodermal ridge (AER)-specific *Fgf8* expression is required for limb patterning (Lewandoski et al., 2000; Moon and Capecchi, 2000). If *Fgf4* and *Fgf8* are deleted in the AER, limb development fails completely, indicating genetic redundancy (Boulet et al., 2004; Sun et al., 2002).

Additionally, from the analyses of expression patterns and experimental manipulations in chick embryos, *Fgf8* may act in other embryonic locations. In presomitic mesoderm, a rostrocaudal gradient of *Fgf8* expression (with higher caudal levels) may define a 'differentiation front' in which presomitic mesoderm becomes segmented as it leaves the *Fgf8* expression domain during axis extension (Dubrulle et al., 2001). Myotome-specific *Fgf8* expression (Crossley and Martin, 1995; Stolte et al., 2002) is implicated in the development of two other somitic subcompartments, the sclerotome (Huang et al., 2003) and the syndetome (Brent et al., 2003). Finally, it has been suggested that FGF8 activity from the nephrogenic cord (NC) of the mesonephros initiates limb bud formation (Crossley et al., 1996; Martin, 1998). Because gastrulation fails in $Fgf8^{-/-}$ embryos, loss-of-function tests of these models require the proper tissue-specific Cre mouse lines for conditional *Fgf8* deletion (Lewandoski, 2001).

Fgf8 expression has also been detected in primitive nephronic structures, although there has been no exploration into its role (Mahmood et al., 1995). In the developing urinary tract, the mesodermally derived Wolffian duct (WD) induces a wave of tubule formation in the adjacent NC to generate the

mesonephros as the WD extends caudally, and *Fgf8* is expressed in these tubules (Crossley et al., 1996; Fernandez-Teran et al., 1997; Vogel et al., 1996). Development of the metanephros begins as the WD reaches the cloaca. There, it develops a diverticulum called the ureteric bud (UB), which grows into the surrounding metanephric mesenchyme (MM) to produce the collecting duct network and to induce mesenchymal-epithelial conversion of MM beneath the UB tips. The conversion of MM is defined by a series of morphogenetic stages, involving condensation and pretubular aggregation (renal vesicles), then tubular aggregation (comma- and S-shaped bodies) and eventual formation of the various epithelial segments of the nephron, including glomerular epithelium and proximal/distal tubules. Genetic targeting studies have, thus far, implicated only a few genes expressed by the MM that are critical to nephron differentiation (reviewed by Perantoni, 2003). Of these, arguably only *Wnt4* is essential for the normal conversion of MM to the epithelia of the nephron (Stark et al., 1994).

To examine the function of *Fgf8* in mesodermal lineages, including the metanephros, we have produced and characterized a transgenic mouse line in which a Cre transgene is driven by the *T* (brachyury) promoter (Clements et al., 1996). This promoter is active in the primitive streak, allowing us to use T-Cre mice to delete a conditional *Fgf8* allele in the mesodermal lineage. We report no *Fgf8* requirement for somitic segmentation, differentiation of somitic subcompartments, or limb bud initiation. However, we discover a major role for *Fgf8* in metanephric development. Like *Wnt4*, *Fgf8* is expressed in the condensing MM during normal development, and its conditional loss causes severe renal hypoplasia. *Fgf8* inhibits apoptosis in the MM and acts in combination with *Wnt4* to sustain *Lim1* expression, which is required for normal nephrogenesis (Kobayashi et al., 2005).

Materials and methods

Production of mutant embryos and β-gal staining

T-Cre transgenic lines were produced by standard pronuclei injection techniques using zygotes derived from crossing B6C3 F1/NCr females to B6C3 F1/J males. Mice carrying various *Fgf8* alleles were maintained on a CD1 background and genotyped as described (Meyers et al., 1998). Generation, maintenance and genotyping of the *Wnt4*$^{-/-}$ line has been described (Stark et al., 1994). β-Galactosidase (β-gal) staining was performed as described (Chi et al., 2003).

In situ hybridization (ISH)

Embryos or dissected urogenital tracts were fixed and processed for whole-mount ISH as described (Pizard et al., 2004). For paraffin-wax embedding, mutant and control metanephroi were fixed as described (Karavanova et al., 1996). Thin section ISH was performed as described (Wilkinson and Green, 1990), using ^{35}S-labeled probes.

Immunohistochemistry (IHC)

For whole-mount IHC, isolated metanephroi were processed as described (Yoshino et al., 2001). UBs were visualized with a rabbit polyclonal pan-cytokeratin antibody (Santa Cruz) at 1:50 and FITC-labeled anti-rabbit IgG antibody at 1:100. For thin sections, deparaffinized tissues were probed with a rabbit polyclonal Cited1 antibody (NeoMarkers) at 1:200, and visualized with a Vectastain ABC kit according to the manufacturer's recommendations.

Proliferation/apoptosis studies

Proliferation was analyzed by examining histone H3 phosphorylation using a rabbit polyclonal antibody against the Ser10 phosphopeptide of histone H3 (Upstate). Cell death was examined with confocal laser microscopy of kidneys stained with LysoTracker Red (Invitrogen) (Zucker et al., 1999).

RNA preparation and microarray analysis

Metanephroi were dissected from E12.5 or E14.5 embryos. For E12.5 control and mutant embryos, MMs and UBs were isolated as described (Karavanova et al., 1996). Tissues were either snap frozen on dry ice, or incubated in Hams F12:Dulbecco's MEM (50:50) with or without FGF8B (200 ng/ml) for 4 hours, and then stored at –70°C. Total RNA was isolated from tissues using Trizol Reagent (Invitrogen), and an RNeasy kit (Qiagen). Total RNA (1-2 μg) was used in cDNA synthesis, and biotinylated cRNA was subsequently generated using the manufacturer's protocols (Affymetrix). Microarray hybridizations to GeneChip Mouse Expression Set 430A and measurement of hybridization intensities were performed and analyzed according to the manufacturer's methods (Affymetrix). Duplicate sets of GeneChips were used to allow statistical evaluation (*t*-test and Change Call).

Tissue explant/recombination studies

For recombination studies, caudal portions of spinal cord (SC) from the E11.5 embryos were stripped of somatic mesoderm and placed on type IV collagen-coated filters in direct contact with isolated MMs. Filters were floated on culture medium (50:50 DMEM:HamsF12) with 10% fetal bovine serum and evaluated grossly for tubule formation at 3 and 6 days. Mutant and control SCs were equally efficient at inducing tubule formation in control MMs, and equally inefficient at inducing tubules in mutant MMs.

Results

Characterization of T-Cre mice

Because T expression in the primitive streak (Wilkinson et al., 1990) coincides with the early *Fgf8* expression domain, we reasoned that T-driven Cre expression would delete a conditional *Fgf8* allele in this region. A T-Cre transgene was constructed using a characterized 500-bp T promoter (Clements et al., 1996) (Fig. 1A). We evaluated 12 T-Cre transgenic lines by examining the β-galactosidase (β-gal) pattern of embryonic progeny derived from T-Cre males crossed to female mice homozygous for the Rosa26R Cre reporter (Soriano, 1999) (Fig. 1B). One line, hereafter referred to as the T-Cre transgenic line and used in all subsequent experiments, displayed a specific recombination pattern, whereas others generated relatively non-specific patterns.

At E6.5, no β-gal activity is evident in embryos heterozygous for both R26R and T-Cre (TCre; R26R) (data not shown). At E7.5, recombination is evident primarily in the primitive streak and migrating mesoderm (Fig. 1C). At E8.0, recombination is widespread in mesodermal lineages, including the allantois (see Fig. 1F), but is mostly absent in the node (Fig. 1D and data not shown). A dorsal view of an E8.5 embryo demonstrates extensive recombination in paraxial, intermediate and lateral mesoderm, but not in neural tissues (Fig. 1E). At E9.0, most mesodermal lineages are β-gal+, but recombination is incomplete in the heart (Fig. 1F). At this stage, recombination is evident at midaxial levels in the notochord and neural tube floorplate, but is absent in gut endoderm (Fig. 1G). More caudally, recombination is extensive

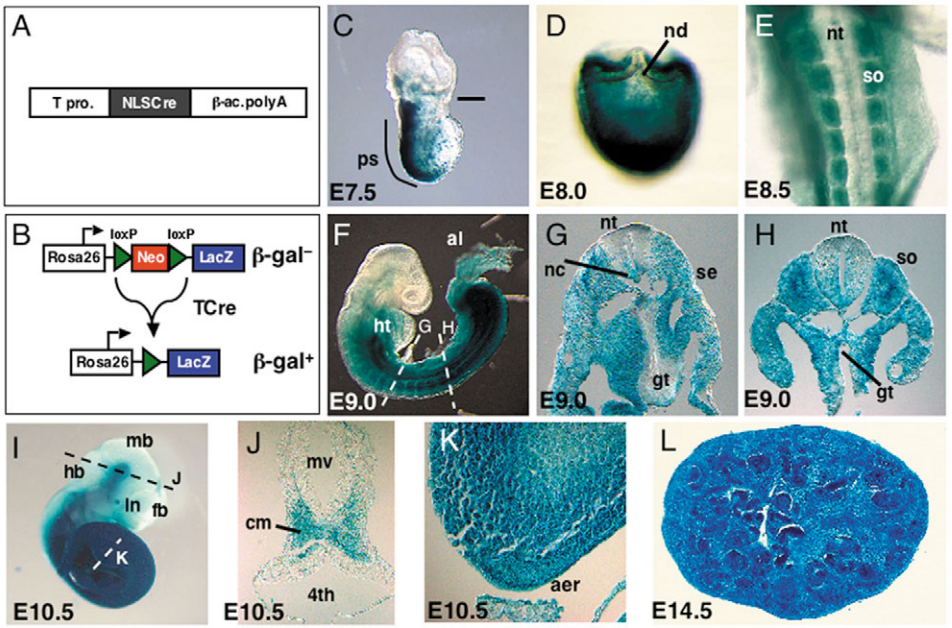

Fig. 1. T-Cre-mediated activation of the R26R reporter allele. (A) Schematic representation of the T-Cre transgene. (B) Cre-mediated recombination of the R26R reporter deletes the *neo*^{R} fragment thereby restoring β-galactosidase activity (β-Gal). (C-L) Whole-mount images (C-F,I) or sections (G,H,J-L) of T-Cre; R26R embryos stained for β-Gal. (C) Lateral view of an E7.5 embryo. Horizontal bar indicates the extraembryonic/embryonic border. (D) Ventral view of an E8.0 embryo, demonstrating reduced staining in the node region. (E) Dorsal view of an E8.5 embryo. (F) Lateral view of an E9.0 embryo. Dotted lines indicate transverse sections shown in panels G and H. (I) Lateral view of an E10.5 embryo. Dotted lines indicate sections in panels J and K. (J) Horizontal section through an E10.5 head. (K) Transverse section through an E10.5 embryo, demonstrating β-Gal staining in the ectoderm and AER. (L) Section through an E14.5 kidney. 4th, fourth ventricle of neural tube; aer, apical ectodermal ridge; al, allantois; β-ac. polyA, DNA fragment containing the β-actin polyA sequences; cm, cephalic mesenchyme; fb, forebrain; gt, gut; hb, hindbrain; ht, heart; ln, lens; mb, midbrain; mv, mesencephalic vesicle; nc, notochord; nd, node; nt, neural tube; pro, promoter; ps, primitive streak; se, surface ectoderm; so, somites.

in neural tube and gut endoderm (Fig. 1H and data not shown), creating a gradient with higher levels in more posterior positions. Recombination is also mostly absent in surface ectoderm (Fig. 1G,H). By E10.5, Cre has activated R26R in the lens (Fig. 1I). A horizontal section through the E10.5 head reveals that *lacZ* has been extensively activated in head mesenchyme, but only marginally in neuronal epithelium (Fig. 1J). Also, recombination has occurred in posterior surface ectoderm, as shown in the hindlimb AER in Fig. 1K. Finally, the examination of sections through an E14.5 kidney demonstrates that all metanephric tissue is recombined (Fig. 1L). Thus, T-Cre recombination and *Fgf8* mesodermal expression domains overlap sufficiently to use this Cre transgenic line to study the effects of *Fgf8* inactivation in mesoderm.

Characterization of T-Cre-mediated deletion of *Fgf8*

To generate embryos lacking *Fgf8* in T-Cre expressing domains, we used the genetic cross shown in Fig. 2A, in which T-Cre; *Fgf8*$^{Flox/\Delta 2,3}$ progeny (or 'mutants') are generated at a 50% frequency, with the remaining T-Cre; *Fgf8*$^{Flox/+}$ progeny serving as controls. We assessed *Fgf8* inactivation by in situ hybridization (ISH) using a probe that hybridizes to wild-type *Fgf8* transcripts but not to transcripts generated from the Cre-derived *Fgf8*$^{\Delta 2,3}$ allele (Fig. 2B). At E6.5, *Fgf8* mRNA was detected in the mutant epiblast in its normal domain, albeit at a slightly reduced intensity (Fig. 2C). By E7.5, *Fgf8* expression was mostly absent, being detectable only at very low levels in the mutant primitive streak (Fig. 2D). At E8.0-8.5, *Fgf8* RNA was absent from mesodermal domains in the primitive streak and cardiac progenitors, but was expressed normally in the neuroepithelium (Fig. 2E,F). At E9.5, *Fgf8* expression was not detected in any of the mesodermal lineages, including the somites and the presomitic mesoderm/tailbud region (Fig. 2G), but it remained in neural structures, such as the mid/hindbrain isthmus, and the surface ectodermal regions, such as the limb bud AER (Fig. 2G).

Fgf8 is not required for somitogenesis, somite differentiation or limb bud induction

We examined mutants for aspects of embryogenesis proposed to be under *Fgf8* control, including somitogenesis (Dubrulle et al., 2001), somite differentiation (Brent et al., 2003; Brent and Tabin, 2004; Huang et al., 2003) and early induction of the limb bud (Crossley et al., 1996). Throughout development somites formed normally (Fig. 2G, see also Fig. S1 in the supplementary material) despite the lack of *Fgf8* expression in the presomitic mesoderm. Furthermore, no defects were observed in any aspect of skeletal development, including the ribs (Fig. S1B,D,G in the supplementary material), which were thought to require myotomal *Fgf8* expression (Huang et al., 2003). To test whether myotomal *Fgf8* expression was required to maintain the tendon progenitor population in the syndetome subcompartment of the somite, we performed ISH for scleraxis, an early marker of this lineage (Brent et al., 2003). Scleraxis expression was normal from E10.5 through E14.5 (Fig. S1A-D in the supplementary material), indicating that *Fgf8* is not essential for this aspect of somite differentiation. Finally, we confirmed the observation that NC-specific Fgf8 expression is not required for limb bud induction (Boulet et al., 2004), as limbs formed at the normal position and time in mutants (Fig. S1E,F in the supplementary material). However, most mutants lacked at least one hindlimb digit (data not shown), presumably because of the Cre-mediated deletion of *Fgf8* in the hindlimb AER (Fig. 1K) (Lewandoski et al., 2000; Moon and Capecchi, 2000).

Fgf8 is required for urogenital development

Mutant offspring appeared normal at birth, but died shortly thereafter and upon dissection showed abnormally small kidneys. Other tissues in the urogenital tract appeared to be grossly and histologically normal, including the adrenals, ureters, bladder and ovaries (Fig. 3A). Accessory tissues in the male reproductive tract, however, were affected, but these alterations will be described in detail elsewhere. Analysis of T-Cre; $Fgf8^{Flox/\Delta 2,3}$ mutants, therefore, provides evidence that the primary requirement for FGF8 in post-primitive streak mesoderm is in kidney development.

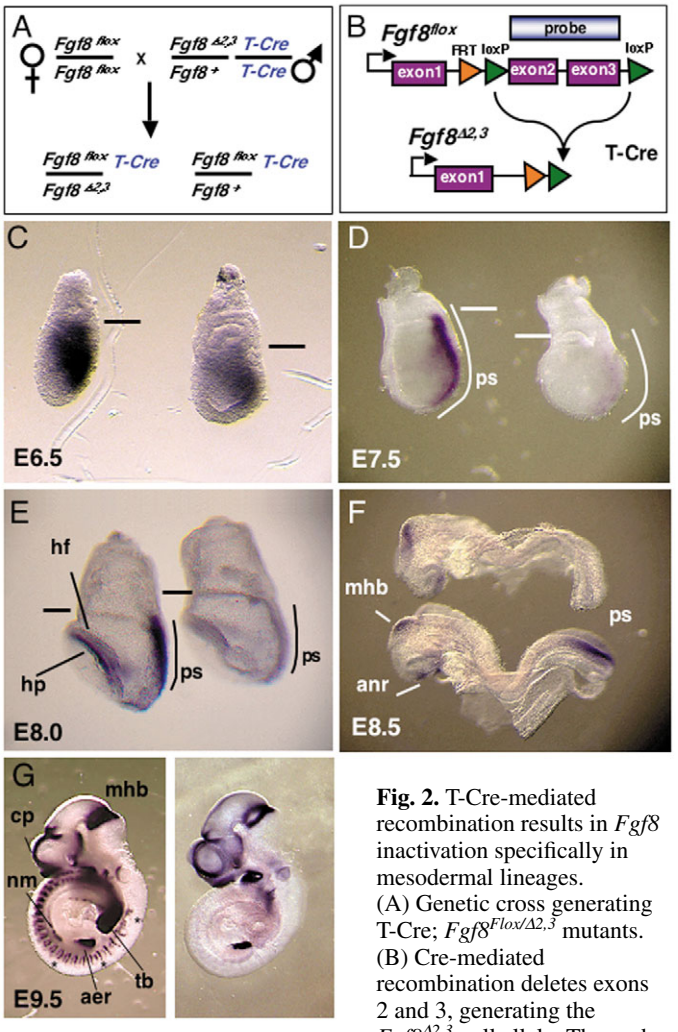

Fig. 2. T-Cre-mediated recombination results in *Fgf8* inactivation specifically in mesodermal lineages. (A) Genetic cross generating T-Cre; $Fgf8^{Flox/\Delta 2,3}$ mutants. (B) Cre-mediated recombination deletes exons 2 and 3, generating the $Fgf8^{\Delta 2,3}$ null allele. The probe indicated was used in ISH of embryos in panels C-G and hybridizes only to mRNA generated from the unrecombined $Fgf8^{Flox}$ allele. (C-G) Lateral views of whole-mount ISH at ages indicated. Mutant embryos are on the right of, or above, the control. *Fgf8* expression is minimally affected in E6.5 mutants (C), but is greatly diminished in E7.5 mutants (D) and absent in E8.0 mutants (E). (F,G) *Fgf8* is expressed in neural epithelium and surface ectoderm structures at E8.5 (F) and E9.5 (G), but is absent in somites (asterisks), tailbud and nephrogenic cord (G). aer, apical ectodermal ridge; anr, anterior neural ridge; cp, commissural plate; hp, heart progenitors; hf, headfold; mhb, mid/hindbrain junction; nm, nephrogenic mesenchyme (cord); ps, primitive streak; tb, tail bud. Horizontal bars indicate the extraembryonic/embryonic border.

Fgf8 expression in the metanephros corresponds with tubule induction

Metanephric development begins at E10.5 with UB formation, growth, and branching in the surrounding MM. The UB induces mesenchymal condensation around it and subsequently causes the condensates beneath its tips to convert to polarized epithelia, which form the renal vesicles and eventually tubules. Concomitant with induction and condensation, *Fgf8* expression occurs in the MM of the E11.5 metanephros beneath the UB tip (Fig. 3B, left) in a ring lining the UB (Fig. 3B, right). At E12.0, *Fgf8* gene expression is localized to distinct pretubular aggregates (Fig. 3C, left). At E14.5, *Fgf8* expression is present in pretubular and comma- and S-shaped bodies, and in glomerular epithelia (Fig. 3D,E). We never detected *Fgf8* expression in the UB or interstitial stroma. Therefore, we hypothesize that *Fgf8*-expressing mesenchymal cells at E11.5 and E12.0 are nephrogenic and not stromal progenitors. During nephron maturation, *Fgf8* expression is downregulated. Thus, its expression is coordinated precisely with induction and tubular morphogenesis.

To ensure that *Fgf8* expression has been eliminated in the metanephros by T-Cre activity at the time of tubule induction, E11.5 and E14.5 kidneys were hybridized using the exon2,3-specific probe (Fig. 2B). As expected, *Fgf8* expression was absent in the mutant metanephros at E11.5 (Fig. 3C) and at E14.5, as branching progresses (Fig. 3F). However, using a longer probe that detects mutant transcripts, we observed focal *Fgf8* expression in control and mutant metanephroi at E14.5 (Fig. 3G), indicating that the absence of *Fgf8* exon2,3-specific transcripts is not due to the loss of *Fgf8*-expressing cells and that *Fgf8* expression is not autoregulatory.

Fgf8 is required for nephron development

Histological examination reveals morphologically similar control and mutant metanephroi at E12.5 (Fig. 4A,B). The UB is comparably branched (see Fig. S2A,B in the supplementary material), and caps of condensed mesenchyme and renal vesicles (arrowheads) are readily apparent at UB tips in both mutants and controls (Fig. 4A,B). By E14.5, cap condensation, tubulogenesis (comma- and S-shaped bodies) and glomerulogenesis have occurred in control metanephroi, whereas mutant kidneys show only condensation and renal vesicle formation (arrowheads, Fig. 4C,D), and dramatically reduced UB branching (Fig. S2C,D in the supplementary material). By E16.5, evidence of cap formation is largely absent and few vesicles remain in the mutant kidneys. Furthermore, vesicles do not progress to form comma- and S-shaped bodies (Fig. 4E,F). At E18.5, the hypocellular mutant rudiment is largely devoid of nephron epithelia, and the remaining few UB radii fail to bifurcate in the cortical nephrogenic region (Fig. 4G,H; Fig. S2E,F in the supplementary material). Interstitial stromal cells populate the increased expanse between UB radii, and hypercellular areas in the nephrogenic zone are limited to regions directly around the UB radii. Glomeruli are absent during any stage of development in mutants, indicating that these kidneys are nonfunctional and that renal failure probably causes neonatal death.

Mutants exhibit aberrant patterns of apoptosis

To understand the biological basis for the aberrant development

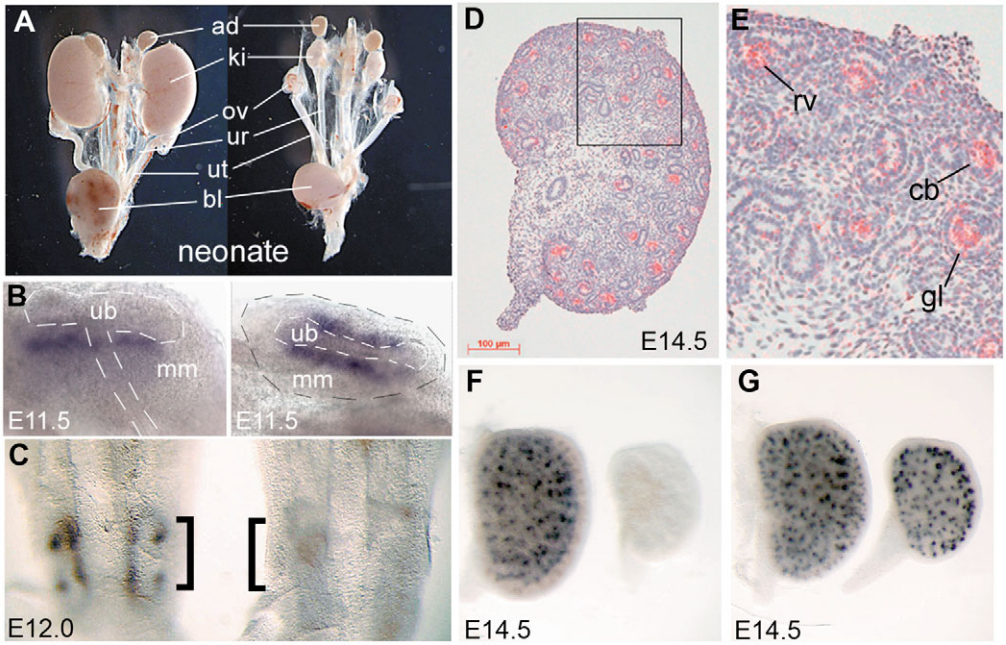

Fig. 3. *Fgf8* expression in control and T-Cre; $Fgf8^{Flox/\Delta 2,3}$ kidneys. (A) Urogenital tissues of control and mutant female neonates showing abnormally small kidneys. (B) Whole-mount ISH of *Fgf8* in a control 11.5 kidney (left, lateral view; right, dorsal view), demonstrating expression adjacent to the ureteric bud. The ureteric bud and kidney are outlined in white and black dashed lines, respectively. (C) Whole-mount ISH using a *Fgf8* probe specific for the Cre-deleted sequences (see Fig. 2B) of the E12.0 urogenital region (ventral view) in control (left) and mutant (right). Brackets indicate kidneys. (D) ISH performed on sectioned E14.5 control kidney. (E) Enlargement of the box in D illustrates *Fgf8* expression in renal vesicles and newly formed tubules. (F) Whole-mount ISH using a *Fgf8* probe specific for Cre-deleted sequences (see Fig. 2B), demonstrating expression in control (left) and mutant (right) E14.5 kidneys. (G) Whole-mount ISH using an *Fgf8* probe including sequences outside of the Cre-deleted region (see Fig. 2B), demonstrating continued *Fgf8* expression of Fgf8 in both control (left) and mutant (right) E14.5 kidneys. ad, adrenal gland; bl, bladder; cb, comma-shaped body; gl, glomerulus; ki, kidney; mm, metanephric mesenchyme; ov, ovary; rv, renal vesicle; ub, ureteric bud; ur, ureter; ut, uterus.

and decreased size of the kidney at E14.5 and E16.5, we compared cell proliferation and death in mutant and control kidneys. No apparent differences in proliferation were detected at E12.5, 14.5 and E16.5, as determined by immunostaining for phosphorylated histone H3 (see Fig. S3 in the supplementary material), which marks mitotic cells (Gurley et al., 1978). Also, the extent of cell death in E12.5 mutant metanephroi, as determined by staining with the fluorophore Lysotracker Red (Fig. 5) or TUNEL assay (not shown), was similar to control tissues. Apoptotic cells were localized primarily to the interstitial stroma and were not associated with mesenchyme in the cortical nephrogenic zone or in condensates (Fig. 5A,B). Cell death, however, was significantly increased in E14.5 (Fig. 5C-E) and E16.5 (Fig. 5F-H) mutant kidneys, where differential staining was most prominent in the cortical mesenchyme (Fig. 5D,G arrows), and, at E16.5, in primitive epithelia (Fig. 5H, arrowheads). Thus, MM-derived cells, especially those in the nephrogenic zone where mesenchymal-epithelial differentiation occurs, depend upon *Fgf8* expression for survival.

To determine whether dying cortical MM cells in mutant tissues were nephrogenic or stromal progenitors, we examined the expression of *Foxd1/BF2*, which localizes to interstitial and cortical stromal populations during nephrogenesis (Hatini et al., 1996), and CITED1, which delineates putative nephrogenic cells in the cap overlying the UB tips in the cortical zone (Plisov et al., 2005). Strong *Foxd1/BF2* expression is observed in the cortical region surrounding epithelial structures at E14.5 (Fig. 6A,B) and E16.5 (Fig. 6C,D) in control and mutant metanephroi, indicating the persistence of the stromal population. These observations were supported by microarray analysis indicating that *Foxd1/BF2* expression levels were increased by more than two times in E14.5 mutants, when compared with control metanephroi (data not shown). For CITED1, mutant expression is diffuse and poorly defined in the cortical MM at E14.5 (Fig. 6E,F), and is significantly depleted at E16.5 (Fig. 6G,H). Furthermore, *Cited1* mRNA levels in E12.5 mutant MMs were decreased compared with controls, and increased with FGF8 treatment (see Table S1 in the supplementary material). These data strongly suggest that nephrogenic and not stromal progenitors were dying as a result of *Fgf8* loss.

Marker gene expression in T-Cre; $Fgf8^{Flox/\Delta 2,3}$ mice

To assess the molecular effects of *Fgf8* loss during metanephric development, we evaluated the expression of mesenchymal and epithelial markers required for metanephric development. The Wilms tumor suppressor *Wt1* is normally expressed at moderate levels in induced and condensed MM, and is upregulated in podocytes (arrows in Fig. 7) (Armstrong et al., 1993). In mutants, no strong focal expression is detected, confirming the histological absence of podocytes/glomeruli. *Nmyc* (*Nmyc1* – Mouse Genome Informatics) and *Pax2* are both highly expressed in condensed mesenchyme and pretubular aggregates of MM in control and mutant E14.5 metanephroi, but are lost from mutant E16.5 MMs (Fig. 7), consistent with the depletion of nephrogenic precursors indicated in our Cited1 studies. By contrast, UB-specific *Pax2* expression persists in mutant and control tissues. UB-limited *Gata3* expression (Lim et al., 2000) occurs in control and mutant E14.5 metanephroi, and demonstrates that epithelial structures under the UB tips in mutants are not of UB origin but rather are renal vesicles. Mutant UBs lose *Gata3* expression by E16.5. The Gdnf-receptor *Ret*, a critical factor

in UB branching and a marker of UB tips, is depleted in mutants at the E14.5 to E16.5 transition (Fig. 7) but is present during early branching. These markers document the precipitous decline of metanephric differentiation between E14.5 and E16.5. Importantly, the decline of *Nmyc* and *Pax2* expression in condensed mesenchyme and pretubular aggregates demonstrates that the precursors for nephron development exist in E14.5 mutant renal anlage but are depleted at E16.5, which is consistent with histological observations.

Identification of early responsive genes for Fgf8 signaling in the developing kidney

To assay for molecular events preceding the morphological changes observed in E14.5 and E16 mutants, we performed microarray analysis on isolated MMs at E12.5, when UB branching and cell death patterns in mutants appear normal. Mutant and normal tissues were evaluated directly upon dissection or, in the case of mutant tissues, some were incubated for 4 hours with FGF8b (200 ng/ml). This permitted identification of immediate-early response genes and also helped to confirm the changes in gene expression profiles observed when comparing genes downregulated in the absence of FGF8 with those induced with FGF8 treatment. Following change call and *t*-test statistical analyses, 31 genes were significantly both decreased in E12.5 mutant MMs and increased with the brief FGF8 treatments (see Table S1 in the supplementary material). Of particular interest were *Egr1* (Rackley et al., 1995), *Nmyc* (Bates et al., 2000), *Lim1* (Kobayashi et al., 2005), and an inhibitor of receptor tyrosine kinases, sprouty 1 (Gross et al., 2003), all of which have been previously implicated in nephrogenesis through mouse genetic analyses. *Wnt4*, which plays a central role in nephron development (Stark et al., 1994), was upregulated in MM after a brief treatment with FGF8, and it was decreased more than 2-fold in mutants when microarray results were confirmed using semi-quantitative RT-PCR (Fig. S4 in the supplementary material).

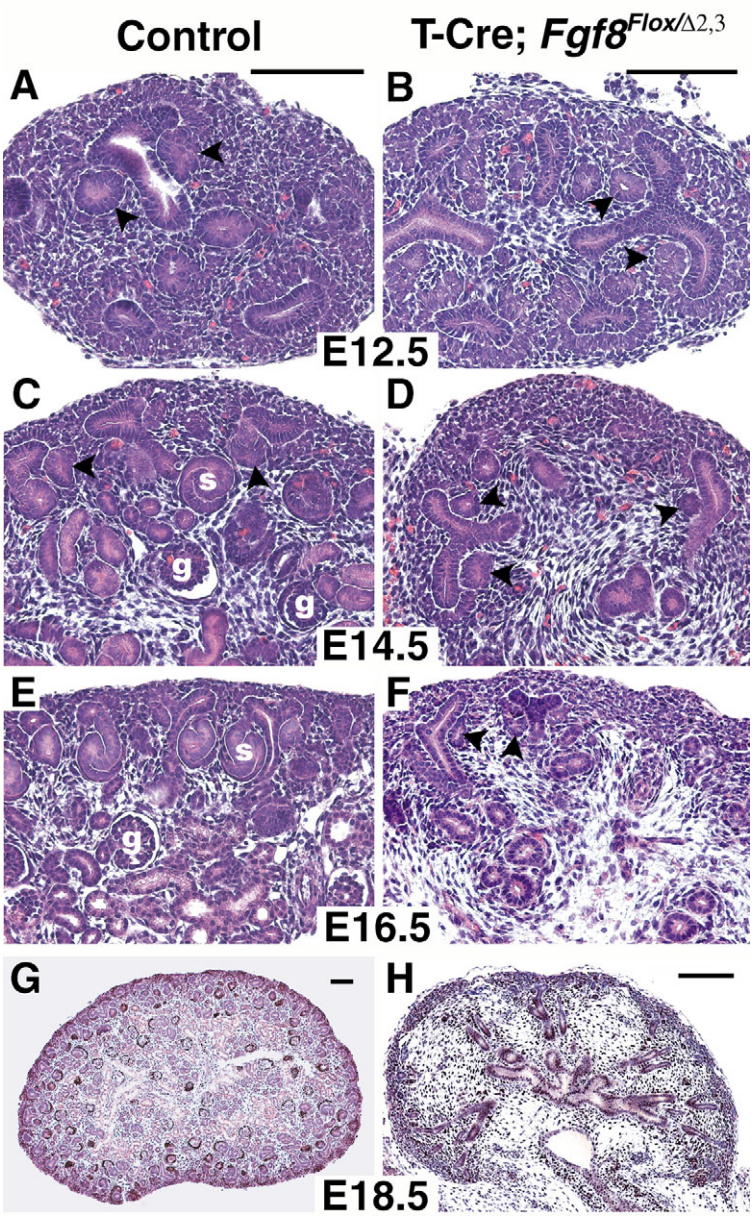

Fgf8 signaling targets both Wnt4 and Lim1

Genetic targeting studies have thus far implicated only a small number of genes expressed by the MM that are crucial to nephron differentiation (reviewed by Perantoni, 2003). Of these, only *Wnt4* activity has been clearly implicated directly in the conversion of MM to the epithelia of the nephron (Kispert et al., 1998; Yoshino et al., 2001), the signature event in renal differentiation. Because *Fgf8* and *Wnt4* are similarly expressed in the developing kidney, and are both required for nephrogenesis, it is possible that these secreted factors cooperate during nephron formation. To address this, mutant metanephroi at E12.5 and E14.5 were probed by ISH for *Wnt4* expression. Consistent with our microarray studies, *Wnt4* expression was downregulated in metanephroi deficient for *Fgf8* expression (Fig. 8A), implicating *Wnt4* as a downstream FGF8 target.

In addition to *Wnt4*, microarray analysis revealed that expression of the homeodomain gene *Lim1* was less than 8% of normal levels in MMs and could be induced 2-fold in FGF8-treated mutant MMs (Table S1 in the supplementary material). Normally, *Lim1* is expressed in the UB and in pretubular aggregates formed from induced MM (Fujii et al., 1994; Karavanov et al., 1998). MM-specific inactivation of *Lim1* results in a failure of renal vesicles to form tubules (Kobayashi et al., 2005). In whole-mount ISH

Fig. 4. Metanephric development in control (A,C,E,G) and T-Cre; *Fgf8*$^{Flox/\Delta 2,3}$ (B,D,F,H) progeny stained with Hematoxylin and Eosin. (A,B) At E12.5, control (A) and mutant (B) kidneys show similar patterns of ureteric bud (UB) branching and induction of metanephric mesenchyme, with condensation and renal vesicle formation (arrowheads). (C,D) At E14.5, mutant kidneys (D) show renal vesicles, which do not progress, unlike controls (C) in which S-shaped bodies (s) and glomeruli (g) are evident. This pattern persists at E16.5 (E,F), and, by E18.5 (G,H), only radii of UB branches remain in mutants (H). Scale bars: 100 μm.

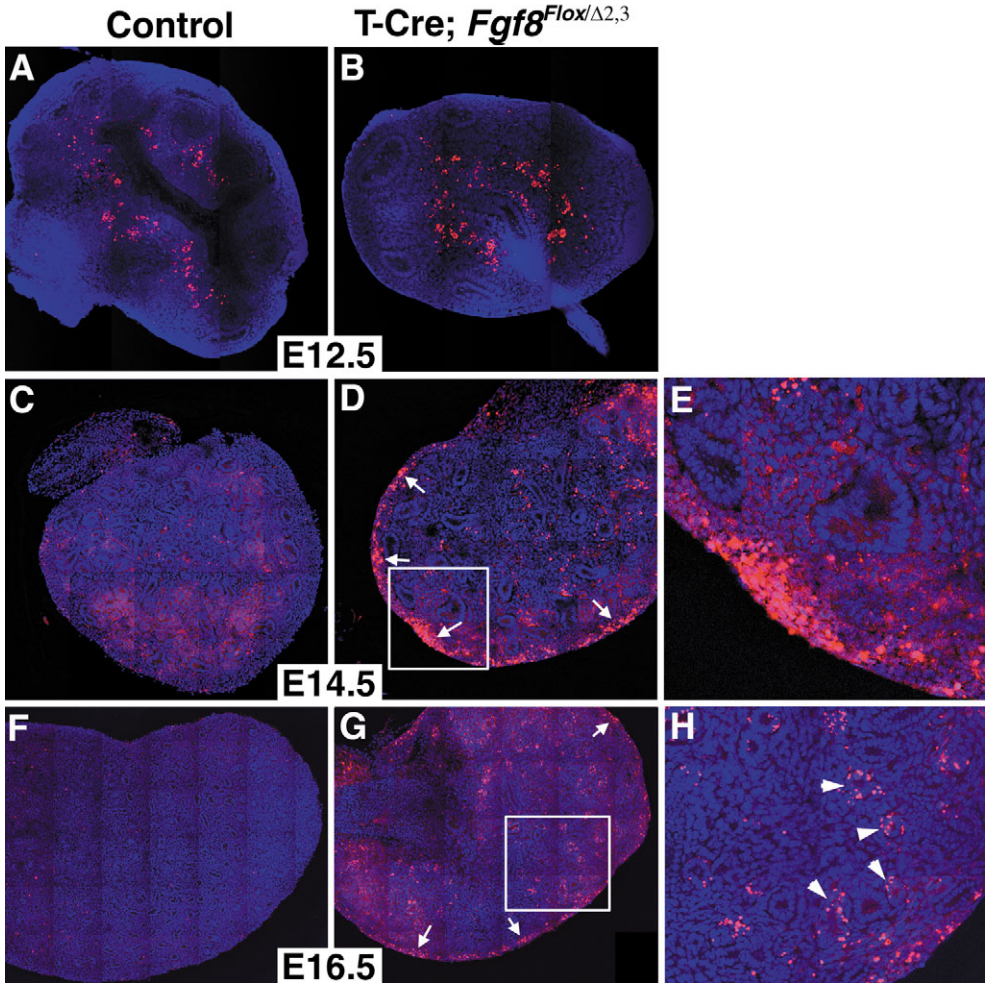

Fig. 5. Aberrant cell death occurs in T-Cre; *Fgf8*$^{Flox/\Delta 2,3}$ kidneys. Confocal imaging of metanephroi from control (A,C,F) or T-Cre; *Fgf8*$^{Flox/\Delta 2,3}$ (B,D,E,G,H) embryos at E12.5 (A,B), E14.5 (C,D,E), E16.5 (F,G,H) stained with the acidotrophic fluorochrome Lysotracker Red. E and H are enlargements of the boxed regions in D and G, respectively. D shows a preferential loss of mesenchymal cells from the cortical nephrogenic zone (also arrows in D and G). H shows a loss of tubular epithelial cells (arrowheads) in mutant tissues.

studies, *Lim1* expression was largely deficient in the MM from E12.5 mutant metanephroi, but was evident in the UB (Fig. 8B,C), thus *Lim1* may function downstream of FGF8 in nephron development.

Loss of Wnt4 results in decreased Fgf8 and Lim1 expression in MM

To further examine the relationship between *Fgf8* and *Wnt4* expression, we evaluated metanephroi from *Wnt4* null homozygotes. Histologically, these tissues resemble the T-Cre; *Fgf8*$^{Flox/\Delta 2,3}$ mutants in that nephron development is largely absent despite branching of the UB in the MM (Stark et al., 1994). In the later stages of development (e.g. E18.5 shown in Fig. 9B), the branched ducts regress to form small numbers of rays that extend into the cortex and are separated by large areas of interstitial stroma as in T-Cre; *Fgf8*$^{Flox/\Delta 2,3}$ metanephroi. However, in contrast to T-Cre; *Fgf8*$^{Flox/\Delta 2,3}$ metanephroi and previously published studies (Stark et al., 1994), we found that a few nephron-like structures form in the absence of *Wnt4* (Fig. 9B). Thus, in the absence of *Wnt4* some tubulogenesis occurs but is severely reduced, resulting in a phenotype that resembles that caused by *Fgf8* inactivation.

Wnt4$^{null/null}$ metanephroi were also subjected to microarray analysis. A comparison with microarray results from T-Cre; *Fgf8*$^{Flox/\Delta 2,3}$ MM (Table S1 in the supplementary material) and intact metanephroi (not shown) revealed some commonality in regulation at E12.5; for example, loss of either *Wnt4* or *Fgf8* caused a decreased expression of *Egr1*, *Nmyc* and *Lim1* by more than 2-fold, which may underlie the common defects shared by T-Cre; *Fgf8*$^{Flox/\Delta 2,3}$ and *Wnt4*$^{null/null}$ metanephroi. Also, *Wnt4*$^{null/null}$ metanephroi showed a significant reduction (>2-fold) in *Fgf8* expression. To establish the distribution of *Fgf8* in the absence of *Wnt4*, E12.5 and E14.5 *Wnt4*$^{null/null}$ metanephroi were probed by ISH. Both whole-mount and thin-section ISH demonstrated focal expression of *Fgf8* in pretubular aggregates from control and mutant tissues. However, numbers of positive foci were reduced in mutants (Fig. 9C-F and data not shown), suggesting that the decreased *Fgf8* expression noted in microarray studies was due to the reduced formation of *Fgf8*-expressing pretubular aggregates. This finding is consistent with a role for *Fgf8* upstream of *Wnt4* expression. A decrease in *Lim1* expression was also noted in microarray studies of *Wnt4*$^{null/null}$ metanephroi (Table S1 in the supplementary material). ISH analysis revealed a loss of *Lim1* expression specifically in populations of MM underlying UB branch termini, but not in the UB itself (Fig. 9H), conforming to the *Lim1* expression pattern observed in the T-Cre; *Fgf8*$^{Flox/\Delta 2,3}$ mutant kidney. Taken together, these data suggest an epistatic relationship in which FGF8 induces *Wnt4*, which plays a major role in nephron formation, possibly through the

induction of *Lim1*. Alternatively, these data are consistent with a model in which FGF8 induces *Wnt4*, and then both WNT4 and FGF8 act in parallel to activate *Lim1* expression and induce tubule formation.

Embryonic inductors require FGF8 to induce tubulogenesis in mutant MM

Explant studies have shown that the incubation of isolated MMs with an inductor such as embryonic spinal cord (SC), which expresses *Wnt1* and other WNT family members, is sufficient to induce tubulogenesis. Furthermore, explanted SC rescues tubulogenesis in *Wnt4*$^{null/null}$ MM (Kispert et al., 1998). Therefore, if *Fgf8* is only required to activate *Wnt4* during nephron formation, then SC explants should also rescue tubule formation in T-Cre; *Fgf8*$^{Flox/\Delta 2,3}$ mutant MM. To test this idea, explanted tissues were co-cultivated for 6 days and evaluated for tubules. In these studies, embryonic SC from either mutant or control embryos induced extensive tubule formation (>20 tubules/explant) at high frequency (93%) in uninduced control MMs isolated from E11.5 metanephroi, often within 3 days (Fig. 10A,B), whereas mutant MMs under similar conditions infrequently (10%) developed tubules (Fig. 10C,D) over 6 days, and then usually <5 tubules/explant (Table S2 in the supplementary material). Thus, normal inductive signaling cannot replace the loss of FGF8 signaling. If FGF8-soaked beads (200 ng/ml), which by themselves are incapable of inducing tubules in explanted MM, were placed on mutant MMs and co-cultivated with embryonic SC, the frequency of tubule formation (75%) was significantly increased (Fig. 10E,F; Table S2 in the supplementary material). These data suggest that the role of FGF8 in tubulogenesis is not simply to activate *Wnt4*, and that FGF8 signaling is required concurrently with WNT4 signaling for tubule formation.

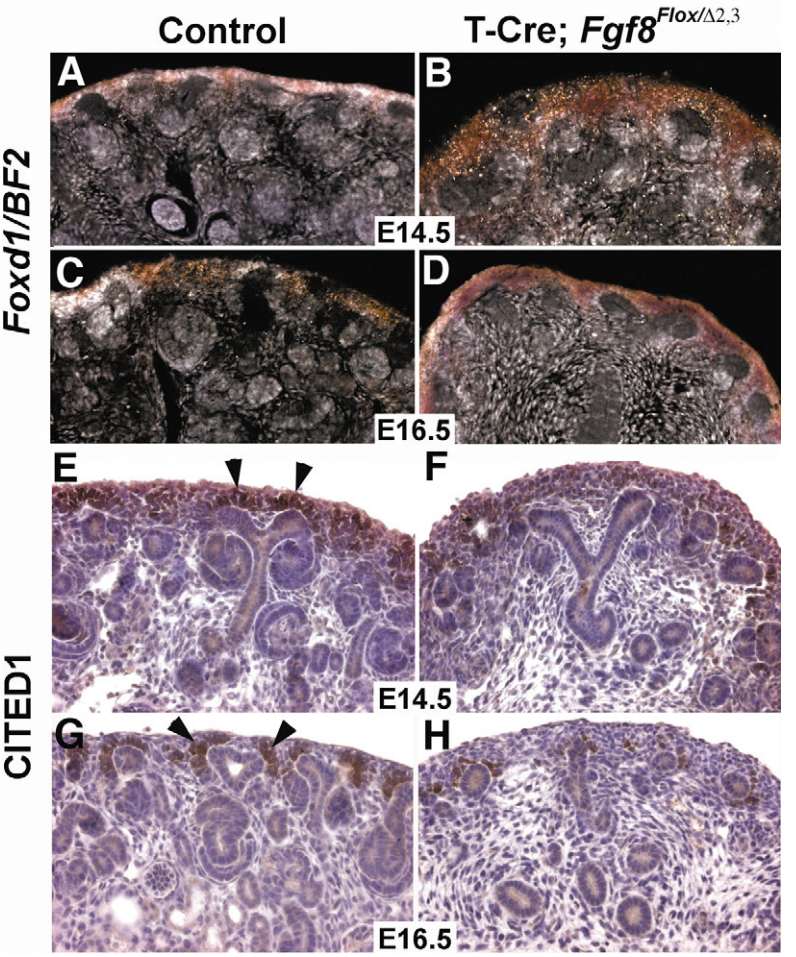

Fig. 6. Nephrogenic progenitors are preferentially lost in T-Cre; *Fgf8*$^{Flox/\Delta 2,3}$ kidneys. (A,B,E,F) E14.5 kidneys; (C,D,G,H) E16.5 kidneys. (A-D) Sustained expression of the stromal marker *Foxd1/BF2* in sections from whole-mount ISH of control (A,C) and T-Cre; *Fgf8*$^{Flox/\Delta 2,3}$ (B,D) metanephroi. (E-H) Depletion of the cap cell marker Cited1 demonstrated by immunohistochemistry of control (E,G; arrowheads indicate cap formation) and T-Cre; *Fgf8*$^{Flox/\Delta 2,3}$ (F,H) metanephroi.

Discussion

We document the effectiveness of a T-Cre transgenic mouse line for site-specific recombination in the emerging mesoderm. T-Cre mice were used to conditionally inactivate *Fgf8*. We report that *Fgf8* is required in nephron formation and that it apparently functions in concert with *Wnt4* to facilitate tubule formation in MM, possibly as a result of inducing *Lim1*. This model is supported by Greishammer et al. (Greishammer et al., 2005), who used a different Cre line to inactivate *Fgf8* specifically in the early MM. Furthermore, we observe that *Fgf8* is not required for limb field induction, thereby supporting the work of Boulet et al. and Fernandez-Teran et al. (Boulet et al., 2004; Fernandez-Teran et al., 1997), or segmentation/somite development, as these processes are unimpaired in mutants.

Given the failure of primary mesoderm migration that occurs in *Fgf8*$^{-/-}$ embryos (Sun et al., 1999), our observation that mutants gastrulate normally demonstrates that the small amount of FGF8 present in mutants is above a threshold requirement at this stage. The observation that segmentation and somitic differentiation are normal in our mutants can be reconciled with existing models by speculating that *Fgf8* function is redundant with other FGF genes, such as *Fgf3*, *Fgf4*, *Fgf5*, *Fgf17* or *Fgf18*, which are all expressed in the primitive streak/tail bud (Hebert et al., 1990; Maruoka et al., 1998; Niswander and Martin, 1992; Wilkinson et al., 1988; Xu et al., 1999). Furthermore, during somite differentiation, *Fgf4* and *Fgf8* are both expressed in the myotome (Crossley and Martin, 1995; Kahane et al., 2001; Niswander and Martin, 1992; Stolte et al., 2002), and may together regulate scleraxis (Brent et al., 2003). Alternatively, as the role of *Fgf8* in segmentation and somitic development has been explored in the chick and zebrafish (Dubrulle and Pourquie, 2004), a perhaps less likely explanation postulates that the *Fgf8* requirement in these processes differs between these organisms and the mouse.

Expression studies and in vitro manipulation suggest that FGFs play a role in nephrogenesis, although, heretofore, murine gene targeting approaches have provided a limited

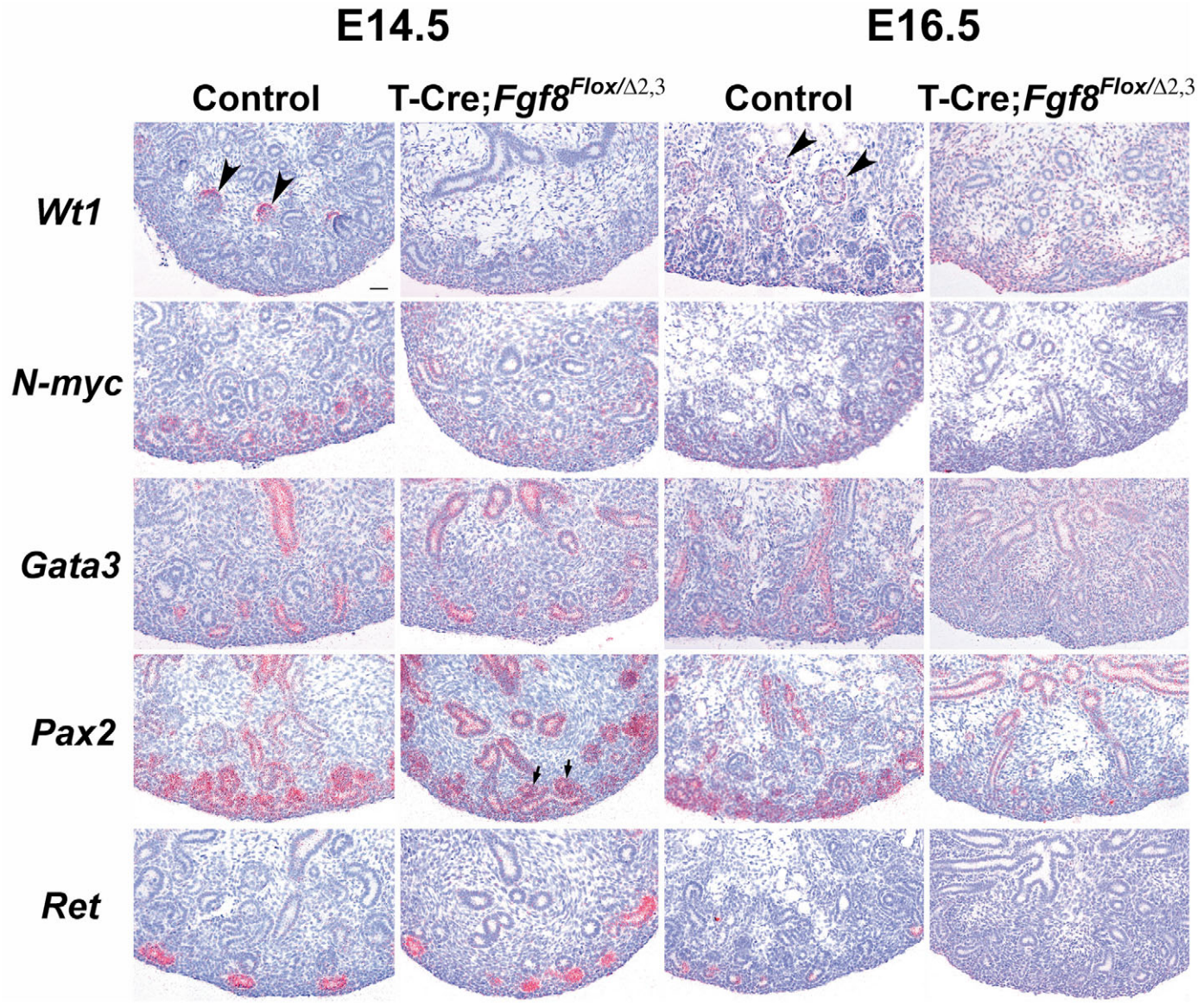

Fig. 7. Substantial loss of multiple metanephric markers occurs in T-Cre; *Fgf8*$^{Flox/\Delta 2,3}$ kidneys between E14.5 and E16.5. Expression patterns for tissue-specific markers of metanephric differentiation in control and mutant E14.5 and E16.5 metanephroi by thin-section ISH. Arrowheads in the *Wt1* panels indicate podocyte expression domains; arrows in the *Pax2* panels indicate renal vesicles. Scale bar: 20 μm.

understanding of their contribution(s) to this process. *Fgf2* is expressed first in the UB during metanephric development and, in explant cultures, induces condensation (Barasch et al., 1997; Perantoni et al., 1995) and some tubule formation in isolated MMs (Karavanov et al., 1998). However, as *Fgf2* null homozygotes have no obvious renal defects (Dono et al., 1998; Ortega et al., 1998), any in vivo role of *Fgf2* must be redundant with other FGF genes, possibly *Fgf9*, which is similarly expressed and also inductive (A.O.P., unpublished). Other FGF genes are expressed by stromal cells in the nephrogenic zone and primarily affect branching morphogenesis (Ohuchi et al., 2000; Qiao et al., 2001; Qiao et al., 1999).

FGF receptor (FGFR) gene expression patterns indicate that nephrogenic progenitors and their derivatives are likely to be competent to respond to various FGF ligands. Expression of all four FGFR genes can be detected in varying degrees in the MM lineage, with *Fgfr1* apparently being expressed the most abundantly and broadly (Grieshammer et al., 2005). Specifically, *Fgfr1* is uniquely expressed in high levels in the cortical zone (Chi et al., 2004; Grieshammer et al., 2005), where nephrogenic progenitors require *Fgf8* for survival. However, T-Cre-mediated inactivation of *Fgfr1* does not phenocopy the T-Cre; T-Cre; *Fgf8*$^{Flox/\Delta 2,3}$ mutant phenotype (X. Sun and M.L., unpublished). Moreover, nephrogenesis is unaffected in mice lacking either *Fgfr3* or *Fgfr4* (Colvin et al., 1996; Weinstein et al., 1998), or the IIIb/IIIc isoforms of *Fgfr2* (Eswarakumar et al., 2002; Revest et al., 2001). Hence it is likely that genetic redundancy exists on the receptor level for FGF signaling within the developing nephron.

We find *Fgf8* expression first in pretubular aggregates at E11.5 in the MM, below the UB at its first bifurcation, and expression is sustained in these and primitive epithelial structures of the

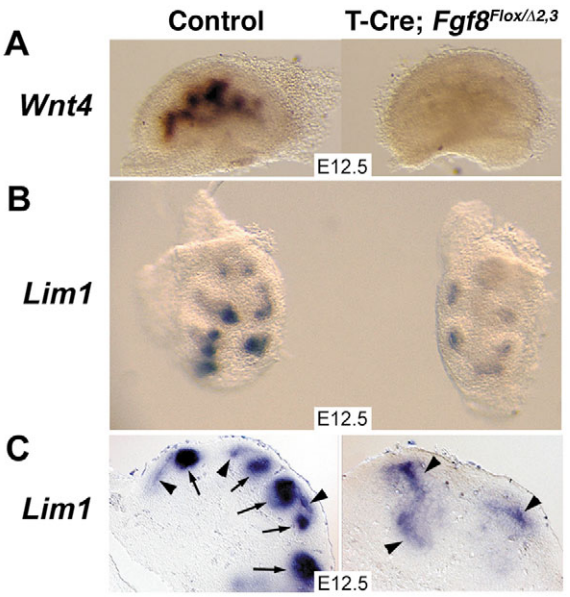

Fig. 8. Prior to phenotypic changes, a loss of *Wnt4* (A) and *Lim1* (B,C) expression occurs in MM in mutant E12.5 metanephroi. Arrows and arrowheads indicate MM and UB expression domains, respectively.

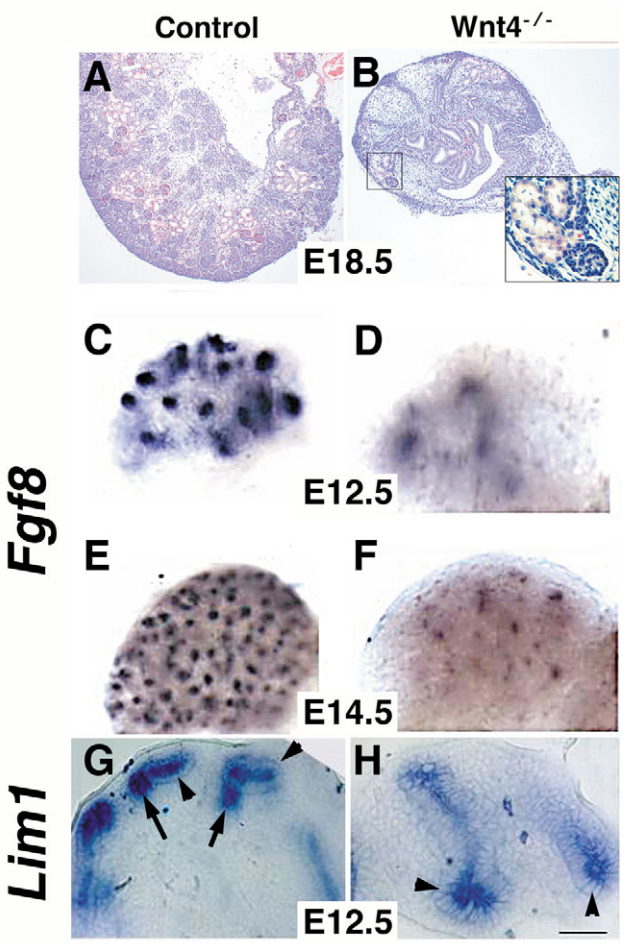

Fig. 9. The *Wnt4*$^{-/-}$ nephrogenic phenotype. (A,C,E,G) Control; (B,D,F,H) *Wnt4*$^{-/-}$. Metanephroi from E18.5 control (A) and *Wnt4*$^{-/-}$ (B) embryos. *Wnt4*$^{-/-}$ metanephroi develop few nephrons (a nephron-like structure is shown in B, inset). (C-H) *Wnt4*$^{-/-}$ metanephroi also develop few foci of *Fgf8* expression (C-E), and express no *Lim1* in induced MM (H, compare with G). Arrows and arrowheads indicate MM and UB expression domains, respectively. Scale bar in H: 250 μm.

nephron. Despite this early expression period, E12.5 mutant metanephroi show normal branching. The presence of appropriate markers for nephron differentiation in condensations and pretubular aggregates of E14.5 mutants, e.g. *Nmyc* and *Pax2*, and the mutant *Fgf8* transcript, indicate that nephrogenic precursors persist at this stage, although histological data demonstrate that this lineage arrests at the renal vesicle stage. This suggests that early stages of metanephric morphogenesis (E12.5) are FGF8 independent, and this is supported by cell death studies, which show no differences between E12.5 mutant and control metanephroi. By E14.5, aberrant apoptotic figures pervade the cortical MM. In addition, there is a depletion of condensed mesenchymal cap cells (and not stromal precursors) that overlay the UB in the cortex and provide precursors for nephron epithelia (Sariola, 2002). On this basis, *Fgf8* may play a role in sustaining nephrogenic mesenchymal progenitors populating the cortical nephrogenic zone – either directly by promoting nephrogenic mesenchyme survival or indirectly through the UB or stroma. By whichever mechanism, the gradual depletion of these progenitors ultimately degrades nephron morphogenesis, which in turn perturbs UB branching, leading to the late loss (E16.5) of *Gata3* and *Ret*, markers of UB morphogenesis. These observations are consistent with previous studies suggesting that FGF8 is a survival factor during development of the first branchial arch (Trumpp et al., 1999), the brain (Chi et al., 2003; Storm et al., 2003), and the limb bud (Moon and Capecchi, 2000; Sun et al., 2002).

In E12.5 mutant kidneys, when there is apparently no morphological change in mutants, microarray analyses of mutant MMs identified significant downregulation of a small number of genes, including *Wnt4* and *Lim1*. Both genes are expressed in the same primitive epithelia that secrete FGF8, and the loss of either causes a severe renal phenotype (Kobayashi et al., 2005; Stark et al., 1994). The current studies provide evidence that FGF8 and WNT4 cooperate functionally to induce nephron formation. Mutants for either gene result in inhibited conversion of MM to primitive tubular epithelia and regressive changes in branching morphogenesis. Furthermore, microarray analyses reveal overlap in expression losses in T-Cre; *Fgf8*$^{Flox/\Delta 2,3}$ and *Wnt4* null mutants, notably the downregulation of *Egr1*, *Nmyc* and *Lim1*. Finally, *Wnt4* null homozygotes also manifest a wave of aberrant cortical apoptosis similar to that observed in T-Cre; *Fgf8*$^{Flox/\Delta 2,3}$ mutants (S.V., unpublished), indicating that WNT4 may stimulate the same population of cortical mesenchyme as does FGF8.

Also, a similar loss of gene expression occurs for *Fgf8* and *Wnt4* in both T-Cre; *Fgf8*$^{Flox/\Delta 2,3}$ mutants and *Wnt4* null homozygotes. In metanephroi lacking either gene, *Wnt4* expression is absent in pretubular and tubular aggregates (this work) (see also Stark et al., 1994), whereas *Fgf8* transcripts are detected, but in fewer foci. Conversely, RT-PCR data revealed that FGF8 can induce *Wnt4* expression. Given the observation that *Wnt4* regulates itself (Stark et al., 1994), expression of *Wnt4* levels capable of inducing tubules in the MM may require

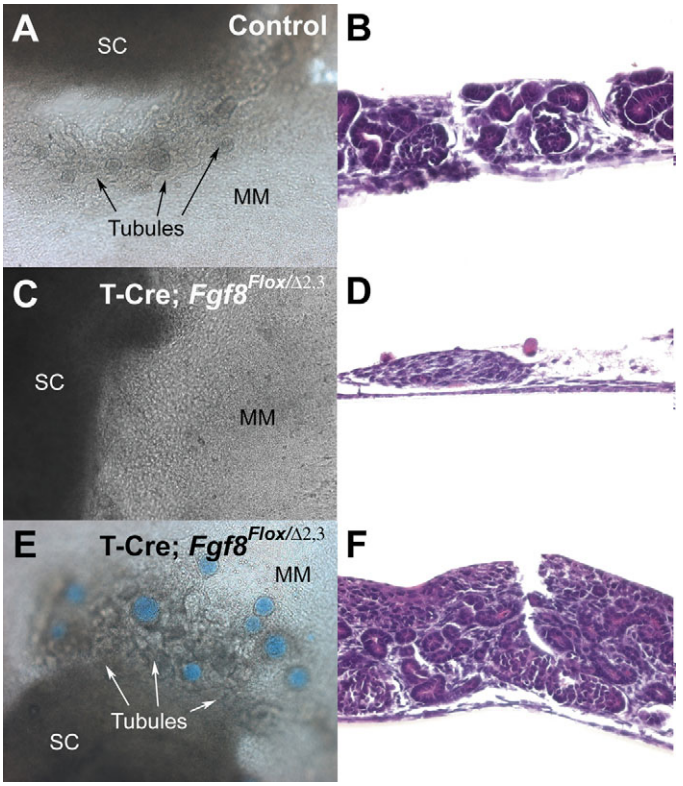

Fig. 10. A Wnt and Fgf8 signal are required for tubulogenesis rescue in mutant MM. (A,C,E) Embryonic spinal cord (SC) induces tubule formation in metanephric mesenchyme (MM) from control embryos (A), but not from T-Cre; *Fgf8*$^{Flox/\Delta 2,3}$ mutant embryos (C) unless Fgf8-soaked beads are added (E). (B,D,F) Sections of cultured tissue shown on the right.

a WNT4 signal in parallel with an FGF8 signal. Taken together, these data support a mechanism in which both *Fgf8* and *Wnt4* cooperate in the progression of MM conversion.

Further support for the hypothesis that FGF8 and WNT4 cooperate in tubulogenesis was provided by tissue co-cultivation studies. When mutant MMs were recombined with embryonic spinal cord, an established WNT source in such experiments, tubule formation was not rescued unless FGF8-soaked beads were added. Thus, a WNT source is not sufficient to induce tubules in MMs, but instead cooperates with FGF8 to induce this morphogenesis. This is reminiscent of the reported co-operativity between *Fgf8* and *Wnt1* in neural development. Similar loss-of-function phenotypes, including patterns of cell death, occur in the mid/hindbrain junction with the loss of *Fgf8* or *Wnt1* (Chi et al., 2003), and each gene is required for the normal regulation of the other (Lee et al., 1997). As suggested, one possibility is that FGF8 and WNT4 act in concert to induce sufficient WNT4 levels. Alternatively, these factors may act on different targets. It is conceivable that WNT4 maintains nephrogenic precursors, while FGF8 is crucial to the progression of renal vesicles to comma- and S-shaped bodies, which is lacking in T-Cre; *Fgf8*$^{Flox/\Delta 2,3}$ mutants.

Nevertheless, despite these phenotypic similarities, some nephron-like structures occur in *Wnt4* null homozygotes but not in T-Cre; *Fgf8*$^{Flox/\Delta 2,3}$ metanephroi. Thus, there is apparently an absolute in vivo requirement for *Fgf8*, but not *Wnt4*, in nephron formation. We speculate that in *Wnt4* null homozygotes, other WNTs (reviewed by Perantoni, 2003; Vainio, 2003) may partially compensate for the lack of WNT4, and, together with FGF8, induce nephron formation. In T-Cre; *Fgf8*$^{Flox/\Delta 2,3}$ metanephroi, which lack both *Fgf8* and *Wnt4* expression, these other WNTs cannot support tubulogenesis.

In addition to early *Wnt4* loss, *Lim1* expression is downregulated at E12.5 in both T-Cre; *Fgf8*$^{Flox/\Delta 2,3}$ and *Wnt4* null homozygous mutants, and is upregulated in *Fgf8*$^{Flox/\Delta 2,3}$ mutant MMs following brief FGF8 treatment. *Lim1* expression is maintained in some mesodermal lineages, including the nephric duct, UB and MM, and MM-specific inactivation of *Lim1* arrests tubulogenesis at the level of renal vesicle development (Kobayashi et al., 2005), as observed in T-Cre; *Fgf8* $^{Flox\ /\Delta\ 2,3}$ mutants. Therefore, FGF8, as well as WNT4, may direct morphogenesis of the MM principally through *Lim1* induction.

Microarray analysis of mutant E12.5 MMs revealed other candidate genes that may also impact on tubular epithelia differentiation. For example, *Nmyc* depletion causes a reduction of cell proliferation in the MM, leading to fewer nephrons (Bates et al., 2000), and inhibition of sprouty 1 gene expression reduces MM condensation in explant culture to decrease nephron numbers (Gross et al., 2003). Thus, several of the genes identified in microarray studies may also contribute in part to the observed phenotype.

However, the loss of *Wnt4* or *Lim1* is apparently sufficient to generate the observed renal phenotype in T-Cre; *Fgf8*$^{Flox/\Delta 2,3}$ mutants. Recombination studies support the concept that both FGF8 and a WNT are necessary to induce tubule formation in MM, although the loss of either gene may affect kidney development by either of two mechanisms. One possibility is that differentiation cannot be sustained due to the loss (through aberrant cell death) of nephrogenic progenitors in the cortical MM and pretubular aggregates. Another possibility is that the pretubular aggregates have lost the capacity to undergo tubular expansion. More likely, both mechanisms are in play; the monitoring of individual populations within the metanephros will delineate the exact role of each factor.

We thank R. Behringer, T. Carroll, G. Martin and E. Meyers for sharing unpublished data, and T. Yamaguchi and Perantoni/Lewandoski lab members for comments on the manuscript. We are grateful to C. Elder (SAIC-Frederick) for excellent mouse husbandry and D. Swing for excellent technical assistance in generating T-Cre transgenic mice. We thank C. Bates, R. Behringer, G. Dressler, J. D. Engel, D. Haber, L. Shen and T. Yamaguchi for ISH probes. We also thank Gian L. Perantoni for excellent technical assistance; Edward H. Cho and Dr Stephen J. Lockett (Image Analysis Laboratory) for the Zeiss LSM510 confocal microscope images; Leslie Mounkes for microscopic assistance; and Jen Matta and Roberta Smith of the Pathology/Histotechnology Laboratory, SAIC-Frederick for tissue sectioning.

Supplementary material

Supplementary material for this article is available at
http://dev.biologists.org/cgi/content/full/132/17/3859/DC1

References

Abu-Issa, R., Smyth, G., Smoak, I., Yamamura, K. and Meyers, E. N. (2002). Fgf8 is required for pharyngeal arch and cardiovascular development in the mouse. *Development* **129**, 4613-4625.

Armstrong, J. F., Pritchard-Jones, K., Bickmore, W. A., Hastie, N. D. and

Bard, J. B. (1993). The expression of the Wilms' tumour gene, WT1, in the developing mammalian embryo. *Mech. Dev.* **40**, 85-97.
Barasch, J., Qiao, J., McWilliams, G., Chen, D., Oliver, J. A. and Herzlinger, D. (1997). Ureteric bud cells secrete multiple factors, including bFGF, which rescue renal progenitors from apoptosis. *Am. J. Physiol.* **273**, F757-F767.
Bates, C. M., Kharzai, S., Erwin, T., Rossant, J. and Parada, L. F. (2000). Role of N-myc in the developing mouse kidney. *Dev. Biol.* **222**, 317-325.
Boulet, A. M., Moon, A. M., Arenkiel, B. R. and Capecchi, M. R. (2004). The roles of Fgf4 and Fgf8 in limb bud initiation and outgrowth. *Dev. Biol.* **273**, 361-372.
Brenner, R. M., Slayden, O. D., Rodgers, W. H., Critchley, H. O., Carroll, R., Nie, X. J. and Mah, K. (2003). Immunocytochemical assessment of mitotic activity with an antibody to phosphorylated histone H3 in the macaque and human endometrium. *Hum. Reprod.* **18**, 1185-1193.
Brent, A. E. and Tabin, C. J. (2004). FGF acts directly on the somitic tendon progenitors through the Ets transcription factors Pea3 and Erm to regulate scleraxis expression. *Development* **131**, 3885-3896.
Brent, A. E., Schweitzer, R. and Tabin, C. J. (2003). A somitic compartment of tendon progenitors. *Cell* **113**, 235-248.
Chi, C. L., Martinez, S., Wurst, W. and Martin, G. R. (2003). The isthmic organizer signal FGF8 is required for cell survival in the prospective midbrain and cerebellum. *Development* **130**, 2633-2644.
Chi, L., Zhang, S., Lin, Y., Prunskaite-Hyyrylainen, R., Vuolteenaho, R., Itaranta, P. and Vainio, S. (2004). Sprouty proteins regulate ureteric branching by coordinating reciprocal epithelial Wnt11, mesenchymal Gdnf and stromal Fgf7 signalling during kidney development. *Development* **131**, 3345-3356.
Clements, D., Taylor, H. C., Herrmann, B. G. and Stott, D. (1996). Distinct regulatory control of the Brachyury gene in axial and non-axial mesoderm suggests separation of mesoderm lineages early in mouse gastrulation. *Mech. Dev.* **56**, 139-149.
Colvin, J. S., Bohne, B. A., Harding, G. W., McEwen, D. G. and Ornitz, D. M. (1996). Skeletal overgrowth and deafness in mice lacking fibroblast growth factor receptor 3. *Nat. Genet.* **12**, 390-397.
Crossley, P. H. and Martin, G. R. (1995). The mouse Fgf8 gene encodes a family of polypeptides and is expressed in regions that direct outgrowth and patterning in the developing embryo. *Development* **121**, 4439-4351.
Crossley, P. H., Minowada, G., MacArthur, C. A. and Martin, G. R. (1996). Roles for FGF8 in the induction, initiation, and maintenance of chick limb development. *Cell* **84**, 127-136.
Dono, R., Texido, G., Dussel, R., Ehmke, H. and Zeller, R. (1998). Impaired cerebral cortex development and blood pressure regulation in FGF-2-deficient mice. *EMBO J.* **17**, 4213-4225.
Dubrulle, J. and Pourquie, O. (2004). Coupling segmentation to axis formation. *Development* **131**, 5783-5793.
Dubrulle, J., McGrew, M. J. and Pourquie, O. (2001). FGF signaling controls somite boundary position and regulates segmentation clock control of spatiotemporal Hox gene activation. *Cell* **106**, 219-232.
Eswarakumar, V. P., Monsonego-Ornan, E., Pines, M., Antonopoulou, I., Morriss-Kay, G. M. and Lonai, P. (2002). The IIIc alternative of Fgfr2 is a positive regulator of bone formation. *Development* **129**, 3783-3793.
Fernandez-Teran, M., Piedra, M. E., Simandl, B. K., Fallon, J. F. and Ros, M. A. (1997). Limb initiation and development is normal in the absence of the mesonephros. *Dev. Biol.* **189**, 246-255.
Fujii, T., Pichel, J. G., Taira, M., Toyama, R., Dawid, I. B. and Westphal, H. (1994). Expression patterns of the murine LIM class homeobox gene lim1 in the developing brain and excretory system. *Dev. Dyn.* **199**, 73-83.
Grieshammer, U., Cebrián, C., Ilagan, R., Meyers, E. N., Herzlinger, D. and Martin, G. R. (2005). FGF8 is required for cell survival at distinct stages of nephrogenesis and for regulation of gene expression in nascent nephrons. *Development*. **132**, 3847-3857.
Gross, I., Morrison, D. J., Hyink, D. P., Georgas, K., English, M. A., Mericskay, M., Hosono, S., Sassoon, D., Wilson, P. D., Little, M. et al. (2003). The receptor tyrosine kinase regulator Sprouty1 is a target of the tumor suppressor WT1 and important for kidney development. *J. Biol. Chem.* **278**, 41420-41430.
Gurley, L. R., D'Anna, J. A., Barham, S. S., Deaven, L. L. and Tobey, R. A. (1978). Histone phosphorylation and chromatin structure during mitosis in Chinese hamster cells. *Eur. J. Biochem.* **84**, 1-15.
Hatini, V., Huh, S. O., Herzlinger, D., Soares, V. C. and Lai, E. (1996). Essential role of stromal mesenchyme in kidney morphogenesis revealed by targeted disruption of Winged Helix transcription factor BF-2. *Genes Dev.* **10**, 1467-1478.
Hebert, J. M., Basilico, C., Goldfarb, M., Haub, O. and Martin, G. R. (1990). Isolation of cDNAs encoding four mouse FGF family members and characterization of their expression patterns during embryogenesis. *Dev. Biol.* **138**, 454-463.
Huang, R., Stolte, D., Kurz, H., Ehehalt, F., Cann, G. M., Stockdale, F. E., Patel, K. and Christ, B. (2003). Ventral axial organs regulate expression of myotomal Fgf-8 that influences rib development. *Dev. Biol.* **255**, 30-47.
Kahane, N., Cinnamon, Y., Bachelet, I. and Kalcheim, C. (2001). The third wave of myotome colonization by mitotically competent progenitors: regulating the balance between differentiation and proliferation during muscle development. *Development* **128**, 2187-2198.
Karavanova, I. D., Dove, L. F., Resau, J. H. and Perantoni, A. O. (1996). Conditioned medium from a rat ureteric bud cell line in combination with bFGF induces complete differentiation of isolated metanephric mesenchyme. *Development* **122**, 4159-4167.
Karavanov, A. A., Karavanova, I., Perantoni, A. and Dawid, I. B. (1998). Expression pattern of the rat Lim-1 homeobox gene suggests a dual role during kidney development. *Int. J. Dev. Biol.* **42**, 61-66.
Kispert, A., Vainio, S. and McMahon, A. P. (1998). Wnt-4 is a mesenchymal signal for epithelial transformation of metanephric mesenchyme in the developing kidney. *Development* **125**, 4225-4234.
Kobayashi, A., Kwan, K. M., Carroll, T. J., McMahon, A. P., Mendelsohn, C. L. and Behringer, R. R. (2005). Distinct and sequential tissue-specific activities of the LIM-class homeobox gene Lim1 for tubular morphogenesis during kidney development. *Development* **132**, 2809-2823.
Lee, S. M., Danielian, P. S., Fritzsch, B. and McMahon, A. P. (1997). Evidence that FGF8 signalling from the midbrain-hindbrain junction regulates growth and polarity in the developing midbrain. *Development* **124**, 959-969.
Lewandoski, M. (2001). Conditional control of gene expression in the mouse. *Nat. Rev. Genet.* **2**, 743-755.
Lewandoski, M., Sun, X. and Martin, G. R. (2000). Fgf8 signalling from the AER is essential for normal limb development. *Nat. Genet.* **26**, 460-463.
Lim, K. C., Lakshmanan, G., Crawford, S. E., Gu, Y., Grosveld, F. and Engel, J. D. (2000). Gata3 loss leads to embryonic lethality due to noradrenaline deficiency of the sympathetic nervous system. *Nat. Genet.* **25**, 209-212.
Macatee, T. L., Hammond, B. P., Arenkiel, B. R., Francis, L., Frank, D. U. and Moon, A. M. (2003). Ablation of specific expression domains reveals discrete functions of ectoderm- and endoderm-derived FGF8 during cardiovascular and pharyngeal development. *Development* **130**, 6361-6374.
Mahmood, R., Bresnick, J., Hornbruch, A., Mahony, C., Morton, N., Colquhoun, K., Martin, P., Lumsden, A., Dickson, C. and Mason, I. (1995). A role for FGF-8 in the initiation and maintenance of vertebrate limb bud outgrowth. *Curr. Biol.* **5**, 797-806.
Martin, G. R. (1998). The roles of FGFs in the early development of vertebrate limbs. *Genes Dev.* **12**, 1571-1586.
Maruoka, Y., Ohbayashi, N., Hoshikawa, M., Itoh, N., Hogan, B. L. and Furuta, Y. (1998). Comparison of the expression of three highly related genes, Fgf8, Fgf17 and Fgf18, in the mouse embryo. *Mech. Dev.* **74**, 175-177.
Meyers, E. N., Lewandoski, M. and Martin, G. R. (1998). An Fgf8 mutant allelic series generated by Cre- and Flp-mediated recombination. *Nat. Genet.* **18**, 136-141.
Moon, A. M. and Capecchi, M. R. (2000). Fgf8 is required for outgrowth and patterning of the limbs. *Nat. Genet.* **26**, 455-459.
Niswander, L. and Martin, G. R. (1992). Fgf-4 expression during gastrulation, myogenesis, limb and tooth development in the mouse. *Development* **114**, 755-768.
Ohuchi, H., Hori, Y., Yamasaki, M., Harada, H., Sekine, K., Kato, S. and Itoh, N. (2000). FGF10 acts as a major ligand for FGF receptor 2 IIIb in mouse multi-organ development. *Biochem. Biophys. Res. Commun.* **277**, 643-649.
Ornitz, D. M. and Itoh, N. (2001). Fibroblast growth factors. *Genome Biol.* **2**, REVIEWS3005.
Ortega, S., Ittmann, M., Tsang, S. H., Ehrlich, M. and Basilico, C. (1998). Neuronal defects and delayed wound healing in mice lacking fibroblast growth factor 2. *Proc. Natl. Acad. Sci. USA* **95**, 5672-5677.
Perantoni, A. O. (2003). Renal development: perspectives on a Wnt-dependent process. *Semin. Cell Dev. Biol.* **14**, 201-208.
Perantoni, A. O., Dove, L. F. and Karavanova, I. (1995). Basic fibroblast growth factor can mediate the early inductive events in renal development. *Proc. Natl. Acad. Sci. USA* **92**, 4696-4700.
Pizard, A., Haramis, A., Carrasco, A. E., Franco, P., López, S. and

Paganelli, A. (2004). *Whole-Mount In Situ Hybridization and Detection of RNAs in Vertebrate Embryos and Isolated Organs*. New York: John Wiley & Sons.

Plisov, S., Tsang, M., Shi, G., Boyle, S., Yoshino, K., Dunwoodie, S. L., Dawid, I. B., Shioda, T., Perantoni, A. O. and de Caestecker, M. P. (2005). Cited1 is a bifunctional transcriptional cofactor that regulates early nephronic patterning. *J. Am. Soc. Nephrol*. **16**, 1632-1644.

Qiao, J., Uzzo, R., Obara-Ishihara, T., Degenstein, L., Fuchs, E. and Herzlinger, D. (1999). FGF-7 modulates ureteric bud growth and nephron number in the developing kidney. *Development* **126**, 547-554.

Qiao, J., Bush, K. T., Steer, D. L., Stuart, R. O., Sakurai, H., Wachsman, W. and Nigam, S. K. (2001). Multiple fibroblast growth factors support growth of the ureteric bud but have different effects on branching morphogenesis. *Mech. Dev.* **109**, 123-135.

Rackley, R. R., Kessler, P. M., Campbell, C. and Williams, B. R. (1995). In situ expression of the early growth response gene-1 during murine nephrogenesis. *J. Urol.* **154**, 700-705.

Revest, J. M., Spencer-Dene, B., Kerr, K., De Moerlooze, L., Rosewell, I. and Dickson, C. (2001). Fibroblast growth factor receptor 2-IIIb acts upstream of Shh and Fgf4 and is required for limb bud maintenance but not for the induction of Fgf8, Fgf10, Msx1, or Bmp4. *Dev. Biol.* **231**, 47-62.

Sariola, H. (2002). Nephron induction revisited: from caps to condensates. *Curr. Opin. Nephrol. Hypertens.* **11**, 17-21.

Shawlot, W. and Behringer, R. R. (1995). Requirement for Lim1 in head-organizer function. *Nature* **374**, 425-430.

Soriano, P. (1999). Generalized lacZ expression with the ROSA26 Cre reporter strain. *Nat. Genet.* **21**, 70-71.

Stark, K., Vainio, S., Vassileva, G. and McMahon, A. P. (1994). Epithelial transformation of metanephric mesenchyme in the developing kidney regulated by Wnt-4. *Nature* **372**, 679-683.

Stolte, D., Huang, R. and Christ, B. (2002). Spatial and temporal pattern of Fgf-8 expression during chicken development. *Anat. Embryol.* **205**, 1-6.

Storm, E. E., Rubenstein, J. L. and Martin, G. R. (2003). Dosage of Fgf8 determines whether cell survival is positively or negatively regulated in the developing forebrain. *Proc. Natl. Acad. Sci. USA* **100**, 1757-1762.

Sun, X., Meyers, E. N., Lewandoski, M. and Martin, G. R. (1999). Targeted disruption of Fgf8 causes failure of cell migration in the gastrulating mouse embryo. *Genes Dev.* **13**, 1834-1846.

Sun, X., Mariani, F. V. and Martin, G. R. (2002). Functions of FGF signalling from the apical ectodermal ridge in limb development. *Nature* **418**, 501-508.

Trumpp, A., Depew, M. J., Rubenstein, J. L., Bishop, J. M. and Martin, G. R. (1999). Cre-mediated gene inactivation demonstrates that FGF8 is required for cell survival and patterning of the first branchial arch. *Genes Dev.* **13**, 3136-3148.

Vainio, S. J. (2003). Nephrogenesis regulated by Wnt signaling. *J. Nephrol.* **16**, 279-285.

Vogel, A., Rodriguez, C. and Izpisua-Belmonte, J. C. (1996). Involvement of FGF-8 in initiation, outgrowth and patterning of the vertebrate limb. *Development* **122**, 1737-1750.

Weinstein, M., Xu, X., Ohyama, K. and Deng, C. X. (1998). FGFR-3 and FGFR-4 function cooperatively to direct alveogenesis in the murine lung. *Development* **125**, 3615-3623.

Wilkinson, D. and Green, J. (1990). *In Situ Hybridization and the Three-Dimensional Reconstruction Of Series Sections*. London: Oxford University Press.

Wilkinson, D. G., Peters, G., Dickson, C. and McMahon, A. P. (1988). Expression of the FGF-related proto-oncogene int-2 during gastrulation and neurulation in the mouse. *EMBO J.* **7**, 691-695.

Wilkinson, D. G., Bhatt, S. and Herrmann, B. G. (1990). Expression pattern of the mouse T gene and its role in mesoderm formation. *Nature* **343**, 657-659.

Xu, J., Lawshe, A., MacArthur, C. A. and Ornitz, D. M. (1999). Genomic structure, mapping, activity and expression of fibroblast growth factor 17. *Mech. Dev.* **83**, 165-178.

Xu, J., Liu, Z. and Ornitz, D. M. (2000). Temporal and spatial gradients of Fgf8 and Fgf17 regulate proliferation and differentiation of midline cerebellar structures. *Development* **127**, 1833-1843.

Yoshino, K., Rubin, J. S., Higinbotham, K. G., Uren, A., Anest, V., Plisov, S. Y. and Perantoni, A. O. (2001). Secreted Frizzled-related proteins can regulate metanephric development. *Mech. Dev.* **102**, 45-55.

Zucker, R. M., Hunter, E. S., 3rd and Rogers, J. M. (1999). Apoptosis and morphology in mouse embryos by confocal laser scanning microscopy. *Methods* **18**, 473-480.